Anode-type double layers in a nonuniform magnetic field

Steven L. Cartier[a] and Robert L. Merlino
Department of Physics and Astronomy, The University of Iowa, Iowa City, Iowa 52242

(Received 21 August 1986; accepted 27 April 1987)

The properties of strong, magnetized, three-dimensional double layers are studied. The double layers are produced by drawing a discharge to a large anode plate located in the diverging magnetic field region of a cylindrical argon discharge. If the anode voltage is sufficiently high, the electrons that are accelerated through the anode sheath may become sufficiently energetic to ionize the background neutral gas and transform the anode sheath into a strong double layer. The resulting conical-shaped structures, which extend outward from the plate, have parallel, oblique, and perpendicular electric field components with respect to the magnetic field. The axial extent of these structures depends on the plate bias voltage, neutral gas pressure, and the magnetic field. At neutral gas pressures of a few millitorr, the double-layer structures are visually apparent because of the enhanced light emission from neutrals excited by the energetic electrons. Color photographs of some of these structures are shown. The scaling of the width of these double layers with electric field components perpendicular to **B** is also investigated.

I. INTRODUCTION

In recent years, considerable attention has been given to the formation of double layers. The research has involved laboratory experiments, observations in space, theories, and computer simulations. Several review articles on this subject are available.[1–6] Double layers consist of two space-charge layers in close proximity, and may be regarded as spatially localized electric fields extending for many Debye lengths, which separate two quasineutral plasmas of differing space potentials. The strong electric fields in these structures can, for example, accelerate particles to high energies and create particle distributions described as beamlike or possibly conical when a magnetic field is present. These distributions can in turn give rise to waves and turbulence. The excitation of some of these plasma instabilities are expected to be greatly influenced by the presence of a magnetic field. The formation and stability of double layers in a magnetic field in which both the ions and the electrons are magnetized have become active areas of research.

Until recently, double-layer experiments (e.g., Coakley and Hershkowitz[7] and Leung *et al.*[8]) were concerned largely with unmagnetized or very weakly magnetized plasmas. The first studies of unmagnetized anode-type double layers can be attributed to Langmuir[9] while weakly magnetized anode double layers have been recently described, for example, by Torvén and Andersson[10] and by Andersson.[11] Andersson[11] found that the magnetic field was of no decisive importance in the formation of double layers, while Torvén and Andersson[10] were not able to form stable double layers in magnetic fields above several hundred gauss. The formation of a double layer from anode sheaths resulting from ionization of the background gas has been considered by Andersson and Sorensen.[12] With anode double layers, ionization on the high-potential side acts as a virtual plasma source. Alternately, source chambers can also be employed so that the particle distributions on either side of a double layer can be controlled independently.[7,8,13–15] Torvén[15] has generated 1 keV double layers in a plasma column with a uniform magnetic field maintained by two gas discharge sources of a differentially pumped triple-plasma device; although the magnetic field strength was very weak.

Sato *et al.*[16] generated very strong double layers ($e\phi/kT_e \sim 2000$) in a double-ended Q machine ($\approx 100\%$ ionized plasma) with a uniform magnetic field of several kilogauss by biasing one hot plate relative to the other. These double layers were, however, one dimensional and thus no information concerning the properties of oblique double layers was obtained. In a novel experiment, Stenzel *et al.*[17] also created a magnetized double layer in which ionization was not a dominant effect by injecting an ion beam into the sheath of a positively biased plate placed in the dipole field of a permanent magnet. Alternately, Jovanović *et al.*[18] created a strongly magnetized double layer in a narrow column by electron beam injection. The potential of the double layers was found to be determined by the electron beam energy. In addition, they found that the characteristic width of the three-dimensional double layers in the direction perpendicular to **B** scaled as the ion gyroradius.

Lennartsson[19] suggested that conical ion distributions may be produced when ions move through oblique double layers. Simulations of two-dimensional double layers in which the orientation of the electric field relative to the magnetic field was varied have been carried out by Borovsky and Joyce.[20–23] They found that the pitch-angle distribution of ions moving through two-dimensional double layers is dependent on the shape and magnetization of these structures. Consequently, these structures may produce energetic ion beams as well as ion conics. Gorney *et al.*[24] have observed both ion conics and ion beams on most satellite passes through the auroral zone. Although Ungstrup *et al.*[25] attribute these distributions to transverse ion acceleration and heating by electrostatic ion-cyclotron waves, ion acceleration by oblique double layers provides a direct way of accounting for these observations. The scale lengths involved

[a] Present address: McDonnell Douglas Corporation, St. Louis, Missouri 63301.

 0031-9171/87/082549-12$01.90

in the formation of the double layers, however, must be considered.

According to Swift[26] and Mozer *et al.*[27] magnetized auroral potential structures scale in the perpendicular direction with the ion gyroradii. Borovsky[20] and Borovsky and Joyce,[21,22] however, contend that to a remarkable degree, the structure of strong double layers is independent of the strength and orientation of a magnetic field. Singh *et al.*[28] argued that the lack of dependence on the magnetic field, reported by Borovsky[20] and Borovsky and Joyce[21,22] resulted because the perpendicular scale length was determined by the scale length of the *imposed* nonuniform perpendicular potential drop. In such a situation, the plasma adjusts to the applied scale length and is not free to adjust to the gyroradius of the ions. In contrast, the simulation results of Singh *et al.*[28] showed that the perpendicular scale length freely adjusts according to the gyroradius of the ions. Also, Lennartsson[29] argued that the double-layer perpendicular scale size can be neither much smaller nor much larger than a typical gyroradius of ions approaching from the high-potential side.

Wagner *et al.*[30] included a slight divergence of the magnetic field lines in a simulation for the auroral region and found that mirroring plays a crucial role in stabilizing the double layers. Also, Andersson[11] has noted that a slight divergence of the magnetic field does affect the stability of the double layers. In general, double layers are known to form at constrictions in plasma chambers, see, for example, Levine and Crawford.[31] In double-layer experiments with an axially nonuniform magnetic field, the parallel potential drop was found to appear near the location of the magnetic mirror point.[32,33] So, in fact, it does appear that the formation of double layers is affected by the presence of a magnetic field.

Following a description of the experimental setup (Sec. II), the properties of strong, three-dimensional, magnetized double layers are presented (Sec. III). These double-layer structures have electric field components perpendicular, oblique, and parallel to the magnetic field. Unlike the auroral double-layer structures, however, the parallel electric field component of the double layers presented here is in the *same* direction as the magnetic field gradient. These double layers are formed by drawing a discharge along magnetic field lines to an anode plate located in the diverging field region of a solenoidal hot filament produced argon discharge. Even when the mean-free path for ionizing collisions exceeds the device dimensions, ionization can still play a crucial role in the formation of double layers, as shown by Torvén and Andersson.[10] The present measurements were made over a wide range of parameters. The dependence of the double layers on the magnetic field, and also the axial variation of the electron distribution on either side of the double layers will be presented. A discussion of the results is given in Sec. IV. A preliminary report of some of the results presented here has already been published[34] as well as the observations of electrostatic ion-cyclotron waves associated with these double layers.[35]

II. EXPERIMENTAL SETUP

The experiment was performed in a cylindrical plasma discharge device shown schematically in Fig. 1. The device

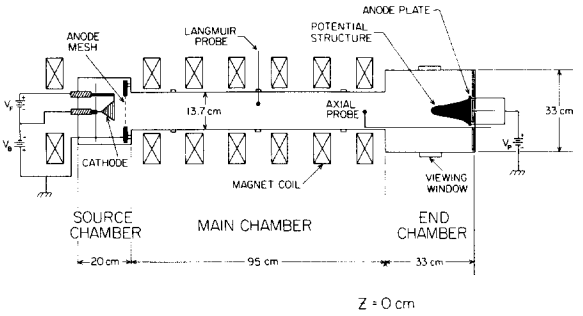

FIG. 1. Schematic cross-sectional view of the experimental setup used to generate double layers. The insert depicts the position and shape of a conical double-layer structure. An arrow indicates the location of $Z = 0$, with Z increasing to the right.

consists of three coaxial chambers with an overall length of ~ 1.5 m. An argon plasma is produced in a stainless steel source chamber by drawing a steady-state discharge current between a directly heated conical spiral tantalum cathode (7 cm in diameter) and a grounded anode stainless steel mesh (20×20 lines/cm). The cathode requires a current of 94 A at about 30 V to produce a discharge of up to 3 A. Typically, the discharge voltage $V_B \simeq 50$–60 V, the discharge current $I_D \simeq 0.5$–1.0 A with argon pressures $P \sim 10^{-4}$ to 10^{-3} Torr. This source produced a 5 cm diam plasma column which was confined radially in the main chamber by a solenoidal magnetic field of up to 7 kG. The plasma density in the central chamber ranged from 10^9 to 10^{11} cm^{-3} with an electron temperature $T_e \sim 1$–3 eV, and with an ion temperature T_i (not measured), believed to range from 0.2 to 0.3 eV, as in similar discharge plasmas. For these parameters the electrons are strongly magnetized $\nu_{en}/\omega_{ce} \ll 1$, whereas the ions are moderately to weakly magnetized $\nu_{in}/\omega_{ci} \lesssim 1$, where $\nu_{e(i),n}$ is the electron (ion)–neutral collision frequency,[36] and $\omega_{ce(i)}/2\pi$ is the electron (ion) gyrofrequency.

This plasma flowed out along diverging magnetic field lines into a large end chamber (33 cm in diameter) as shown in Fig. 1. The magnetic field strength on axis is plotted in Fig. 2, while a few magnetic field lines are indicated in Fig. 3. The plasma is terminated by two electrically isolated metal plates. The larger of these (30 cm in diameter) is mounted on the end wall and is left electrically floating, while the smaller plate (11 cm in diameter) is axially movable and can be biased positively up to $\approx$ 70 V to produce the double-layer structures. Typically, the plate current ranged between 0.5 and 1.0 A, although somewhat higher currents could easily be obtained by adjusting the discharge parameters in the source chamber. The formation of a double layer on the anode plate is depicted by a bell-shaped region shown schematically in Fig. 1 within the end chamber section.

Various electrostatic probes were used to obtain the basic plasma parameters of temperature, density, and potential. In general satisfactory results were only obtained by minimizing probe perturbation effects through the use of very small probes. For cold Langmuir probes, a 0.8 mm in diameter tantalum disk was attached to a tungsten wire insulated with glass tubing (0.18 mm diameter). Similarly, an

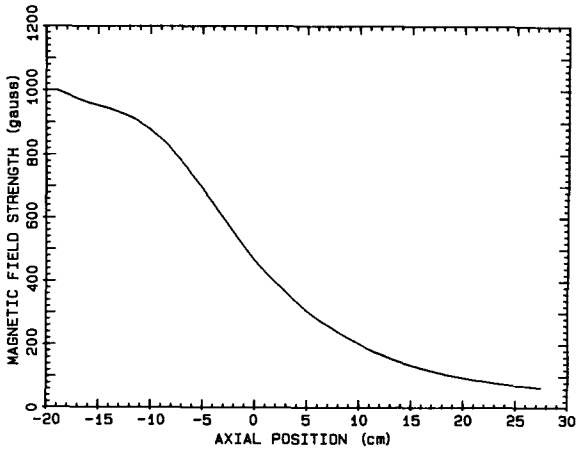

FIG. 2. Plot of the magnetic field strength in the end chamber for $B_{max} = 1.17$ kG.

emissive probe was constructed with a tungsten filament (0.025 mm diameter, 3 mm long) attached to two such glass insulated tungsten wires. The emissive probe was heated using 1.6 V applied across long leads by a battery powered dc voltage regulator. The floating potential of the probe (corresponding to the point at one-half the applied voltage) was used as an approximation of the space potential. For our case, this is an excellent approximation since the floating potential of the emissive probe was typically within 0.5 V of the plasma potential. The full emissive probe characteristic was traced out occasionally to ensure that the measured floating potential was accurately following the plasma potential. Finally, since a visible glow accompanied the double-layer structure, the probes could be observed to ensure that the double-layer structures were not significantly disturbed.

III. EXPERIMENTAL RESULTS

A. General properties of double layers

Stable, three-dimensional, magnetized double layers are generated by applying a positive dc voltage to a large anode plate located in the diverging magnetic field region of the discharge device. As a result, plasma electrons are drawn from the main discharge column along magnetic field lines which map onto the anode plate. At low plate bias voltages, a thin anode sheath forms just in front of the plate. Plasma ions with $T_i \approx 0.2$–0.3 eV are easily reflected at the foot of this sheath. However, when the plate bias voltage is increased to sufficiently high values that the potential drop in the sheath approximately exceeds the background gas ionization potential (15.8 eV for argon), the electrons accelerated through the sheath can become energetic enough to ionize the background gas and so produce a "new" plasma near the anode plate. The ions produced *within* the sheath will in turn act to neutralize part of the electron space charge. If the rate of ionization within the sheath is sufficiently high, part of the anode sheath detaches from the plate and develops into a strong three-dimensional, magnetized double layer.

This effect becomes apparent at anode plate bias voltages generally between 30 and 40 V, although it is dependent on the background neutral gas pressure, with higher plate voltages being required for lower gas pressures. At sufficiently high pressures (above 10^{-3} Torr), a high rate of ionization within the sheath can cause an abrupt increase in the plate current that is associated with a region of negative resistance in the current–voltage characteristic of the plate. This can be seen in Fig. 4, where the plate current I_{plate}, is plotted against plate voltage V_{plate}, for two high-pressure cases. At low biases, the plate current increases before saturating as a result of space-charge effects, but then at biases above about 40 V it rapidly increases once additional electrons are drawn from the newly created plasma. The current–voltage characteristic for lower pressures, however, shows a much more gradual increase in the current with increasing bias voltage.

In addition, at neutral gas pressures above $\sim 10^{-3}$ Torr, the onset of the double layers is accompanied by the appearance of a bluish cone-shaped structure extending from the plate. The sides of this structure form well away from the chamber walls on magnetic field lines slightly inside (~ 1

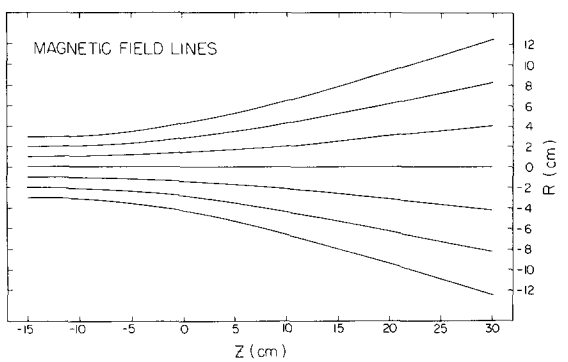

FIG. 3. Lines of constant magnetic flux in the end chamber calculated from the plot shown in Fig. 2.

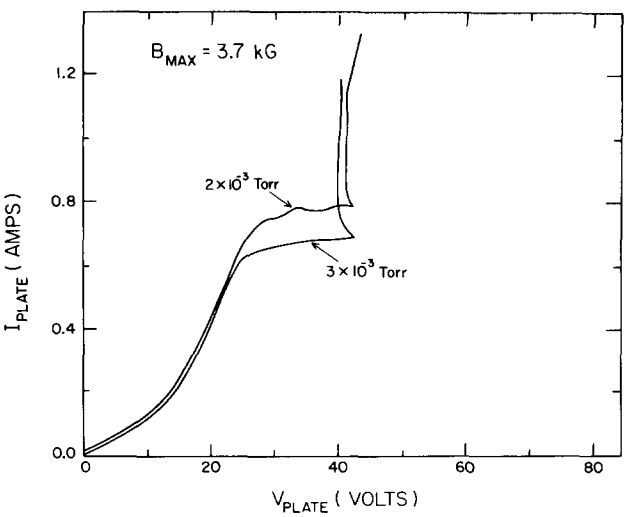

FIG. 4. Current–voltage characteristic of the anode plate. At high pressures, a region of negative resistance appears with the onset of the double layers.

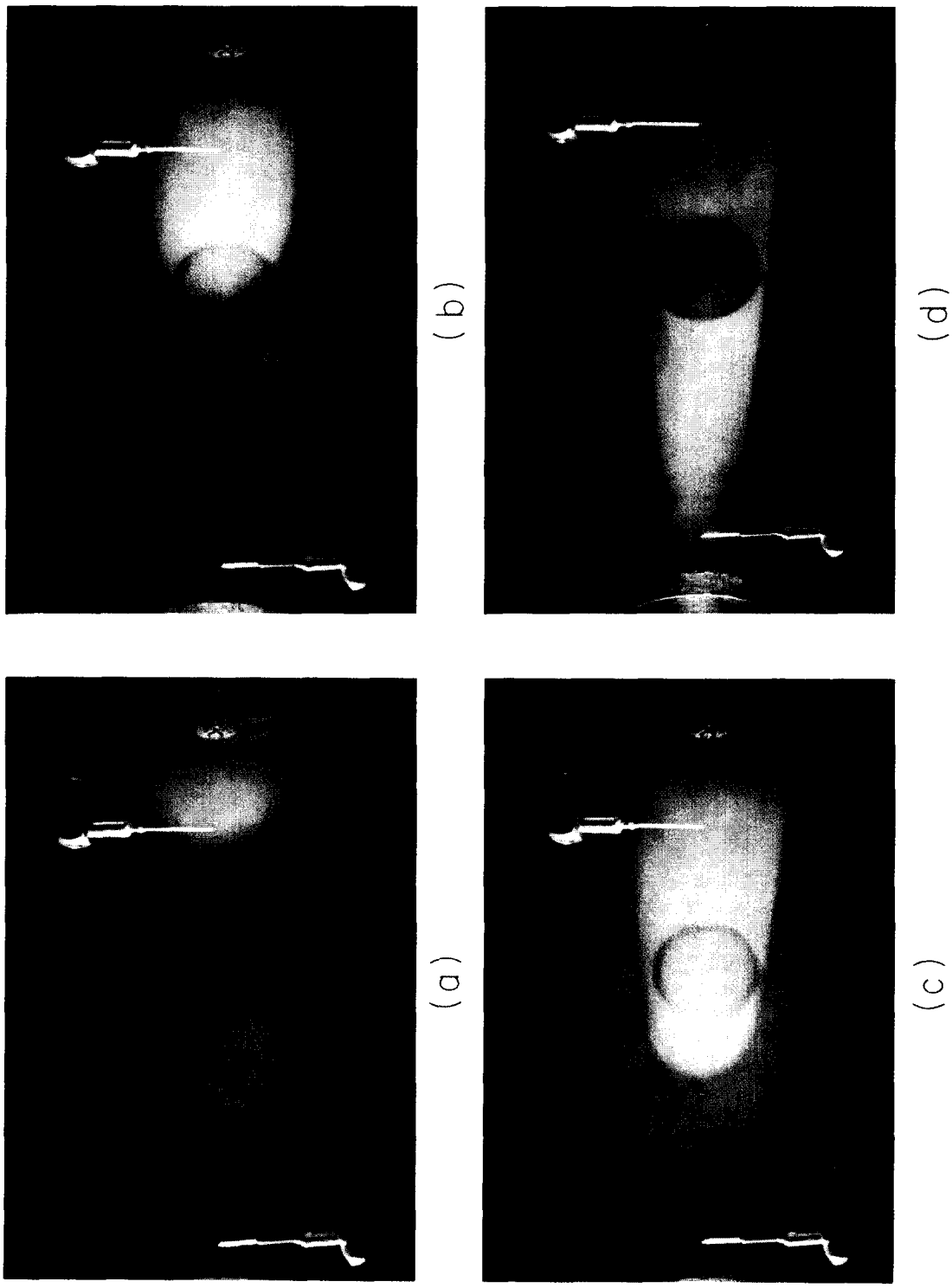

FIG. 5. Sequence of color photographs showing the boundary of the light-emitting region as the anode plate bias voltage is increased. The anode plate appears on the right.

cm) those which map onto the edge of the anode plate. Close examination of these structures, reveals that the light emission comes from a conical shell as thin as a few centimeters. With decreasing pressure, the light emission becomes increasingly more diminished and more evenly distributed throughout the cone. The effect of increasing the anode plate bias voltage beyond the onset value is shown in a series of photographs presented in Fig. 5. The axial boundary of the light-emitting structure, the apex, moves further away from the plate and into the higher magnetic field region with increasing plate bias voltage. In general, for a fixed bias voltage the structure is stable for hours.

Measurements with an emissive probe showed that the visual cone-shaped structures were accompanied by strong double layers. The boundary of the light-emitting region was slightly inside and on the high-potential side of a conical-shaped double layer. This light results from an increased rate of excitation of neutral argon atoms by electrons which had been accelerated through the double layer. In addition, observations of this visual structure indicated that large probes strongly perturbed the measurements. The visual structure can sometimes be seen "following" probes for distances as much as ~ 10 cm.[37] The measured double-layer profiles can appear with a width that is either wider or narrower than the true value, and at the wrong axial position. This effect probably would not, however, be seen by monitoring two probes as mentioned by Coakley and Hershkowitz.[7] This effect seems to occur for any obstacle having dimensions on the order of the ion Larmor diameter, and its effect on the visual surface is greatest when the obstacle is moved through the outside surface of the conical structure, especially ahead of the apex. We were able to minimize this disturbance only by carefully constructing probes with small cross-sectional dimensions.

B. Axial potential profiles

More quantitative measurements of potential are presented in a series of graphs shown in Fig. 6. In each panel, axial floating potential profiles are shown for various anode plate bias voltages ranging from 30 to 60 V. The sequence of panels covers a wide range in neutral gas pressure and, consequently, plasma density. Note that no attempt was made to maintain a constant plasma density. In all cases, the profiles of potential move away from the anode plate (located at $Z = 31.6$ cm) and into higher magnetic field regions with increasing plate bias voltage ($B_{\max} = 3.7$ kG). At neutral gas pressures below about 2×10^{-4} Torr, only extended sheathlike structures are produced. A region where the potential decreases by about 2 V can also be seen. This dip would act to limit the electron current collected by the plate and thus inhibit ionization within the sheath. At higher pressures, double-layer-like structures are more readily produced. At pressures of about 2.5×10^{-3} Torr, a well-defined double layer that is clearly detached from the plate can be produced with only 40 V. The dip in potential seen at lower pressures becomes less apparent with increasing pressure, although it can still be seen in some high-bias cases. At high biases and high pressures, the potential of the plasma ahead of the double layer begins to increase with increasing plate bias voltage until, eventually, the double layer becomes unstable. For even higher biases, intense and sometimes damaging arcs are drawn to the anode plate.

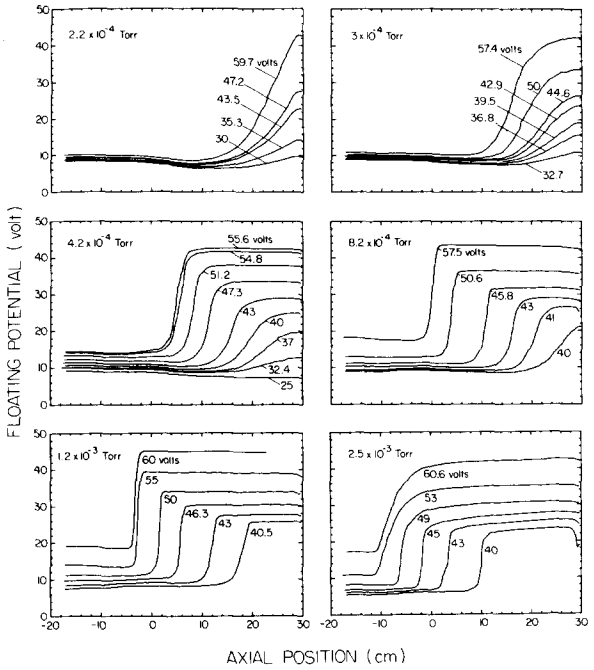

FIG. 6. Double-layer potential profiles ϕ vs Z for various anode plate voltages and neutral gas pressures. The extent of the double layers increases with increasing anode plate voltage.

C. Pressure dependence

The dependence of the double-layer profile on background gas pressure can also be seen in Fig. 7, where the floating potential is again plotted against axial position but for various neutral gas pressures. For this case, the plate bias voltage and the maximum magnetic field strength were fixed at 47 V and 3.7 kG, respectively. It shows that the distance from the anode plate to the double layer increases rapidly with increasing pressure. In addition, Fig. 7 shows that the

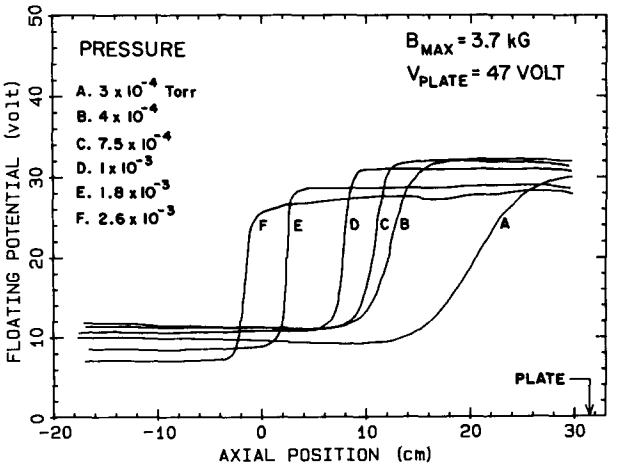

FIG. 7. Double-layer potential profiles ϕ vs Z for various neutral gas pressures with the magnetic field and plate voltage fixed.

width of the double layers $\Delta L_{\parallel}$ appears to decrease with increasing pressure. At 3×10^{-4} Torr, $\Delta L_{\parallel}\sim10$–15 cm, while at 3×10^{-3} Torr, $\Delta L_{\parallel}\sim1$–2 cm. This occurs even though the potential drop across the double layers remains roughly constant, $\Delta\phi\sim20$ V. Both the axial expansion and the steepening of the double layer with increasing pressure can be attributed to an increased ionization probability.

The dependence of plasma density on neutral gas pressure in the absence of a double-layer structure can be seen in Fig. 8. For this case, a Langmuir probe was placed at an axial position $Z = 15$ cm, with the anode plate grounded and the maximum magnetic field strength fixed at 3.7 kG. The electron saturation current I^*_{es}, which is proportional to electron density n_e, is plotted as a function of neutral gas pressure. In the absence of a double layer, the electron density at this particular axial position is found to increase from about 10^8 to 10^{10} cm^{-3}; while the electron temperature remains roughly constant, $T_e = 2.5$–3 eV. This corresponds to a low fractional ionization ratio, typically $n_e/n_n < 0.1\%$, where n_n is the neutral density. When a double layer is produced, the density on the high-potential side is, however, much lower, typically $\sim10^8$ cm^{-3}. At these densities the parallel potential width corresponds approximately to 10–100 electron Debye lengths, i.e., $\Delta L_{\parallel}\sim10$–$100\,\lambda_{De}$, and its dependence on pressure is consistent with the decrease in λ_{De} resulting from the increase in electron density with increasing pressure.

D. Anode voltage dependence

The axial position of the apex for various double layers is shown in Fig. 9 as a function of the anode plate bias voltage.

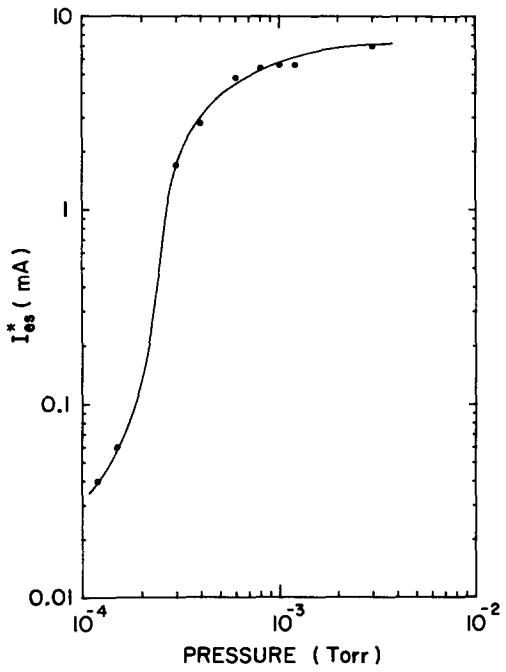

FIG. 8. Electron saturation current drawn to a Langmuir probe located at $Z\sim15$ cm (with the anode plate grounded) as a function of neutral gas pressure. $B_{max} = 3.7$ kG. The plasma density can also be varied by changing the discharge current in the source chamber.

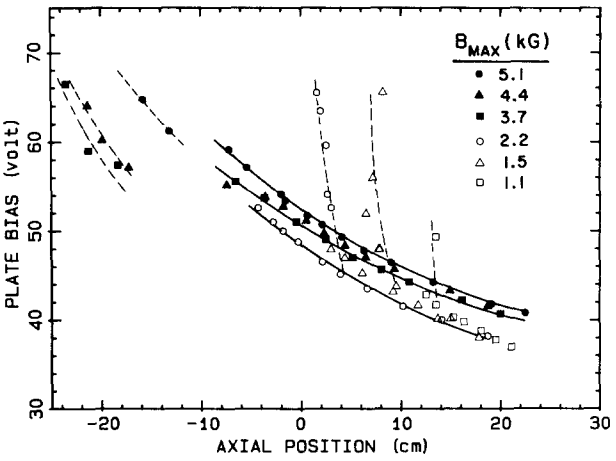

FIG. 9. Axial location of several double layers as a function of anode plate bias voltage for various overall magnetic field strengths.

This was done for several overall magnetic field strengths by using an emissive probe to locate the position where the parallel potential drop across the double layers was about one-half of its full value. For this set, the neutral gas pressure was fixed at $\sim10^{-3}$ Torr. The figure shows that the axial position of the apex of the double layers can be varied over a distance of as much as 45 cm, depending on the overall magnetic field strength. A range in axial locations where no stable double layers can be positioned occurs between -7 and -13 cm. This is also evident by observing the visual light structure which appears to jump across this region as the bias voltage is varied. Figures 2 and 3 show that the magnetic field starts to become uniform at $Z = -9$ cm where the last magnet coil is located. Double layers which are positioned with $Z \lesssim -13$ cm tend to be unstable as is evident by observing the visual light structure which often jumps from one location to another. The dashed lines mark the range of anode bias voltages which cause the potential on the low-potential side of the double layers to rise rapidly with increasing bias voltage. This effect can also be seen in Fig. 6. These

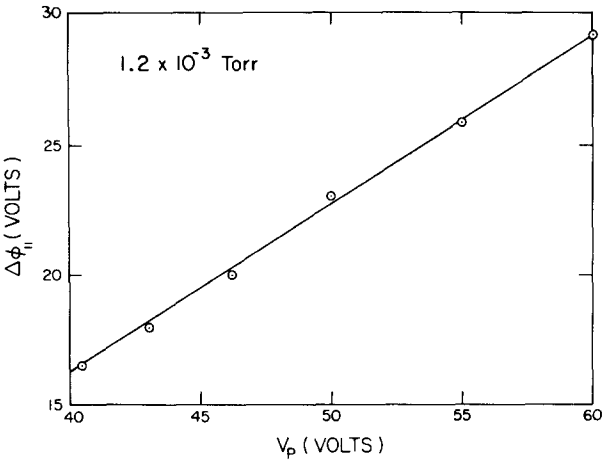

FIG. 10. Parallel potential across the double layer as a function of anode plate voltage for $P\sim1\times10^{-3}$ Torr.

double layers also tend to be unstable and jump occasionally between two locations. Eventually, at high enough biases, frequent localized arcs are drawn to the anode plate.

The dependence of the parallel potential drop across the double layer on the plate bias voltage can be seen in Fig. 10. For pressures of about 10^{-3} Torr, it shows that over the range of applied voltages, the parallel potential across the double layers $\Delta\phi_{\parallel}$ increases linearly from about 16 to 30 V. This corresponds to strong double layers having approximately $e\phi/kT_e \sim 5$–15. It also shows that the double-layer potential is not limited to the argon ionization potential, 15.8 V. The argon ionization cross section is, however, an increasing function of electron energy for the range of energies gained by electrons moving through these double layers. Consequently, the rate of ionization behind these double layers is a function of the double-layer potential drop, as well as the axial distance between the double layer and the anode plate.

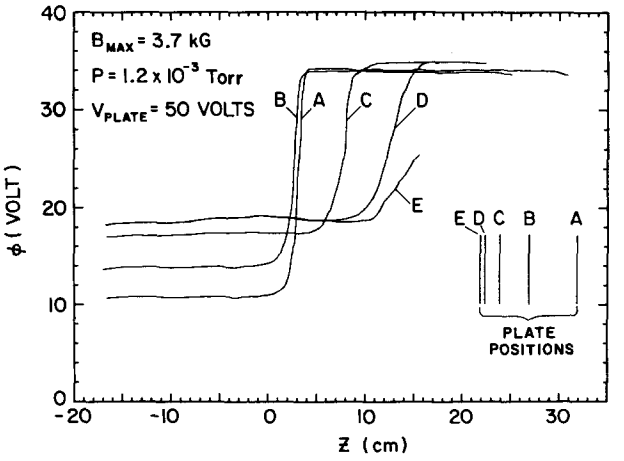

FIG. 12. Axial floating potential profile for several anode plate positions. The double layer collapses when the plate is moved to regions of relatively uniform magnetic fields.

E. Magnetic field strength and anode plate location

Axial double layer potential profiles for various magnetic field strengths are shown in Fig. 11. In this case, the plate bias voltage and the neutral gas pressure were fixed at 45 V and 1.2×10^{-3} Torr, respectively, while the overall magnetic field strength was varied with $B_{\max}$ increasing from 2.2 to 5.1 kG. Over this range of magnetic field strength, the double layer moves toward the plate slightly and its parallel potential drop decreases from 22 to 18 V. Even though the overall magnetic field strength was increased by more than a factor of 2, the field *at the double layer* increased only slightly from 620 to 860 G. For $B_{\max} < 2.2$ kG, this trend is reversed with the double layer moving back towards the plate with decreasing $B_{\max}$. The same effect can also be seen in Fig. 9. For $B_{\max} < 1.1$ kG, the double layer collapses into an anode sheath.

The double-layer profile is also found to depend on the anode plate location as shown by Fig. 12. Here the neutral gas pressure and plate bias voltage were fixed at 1.2×10^{-3} Torr and 50 V, respectively, while the floating potential profile was recorded for several anode plate locations, labeled A to E. As the anode plate is moved into regions where the magnetic field is more uniform and stronger, the double-layer potential decreases and its width broadens, while at the same time the floating potential upstream of the double layer increases. In addition, although the apex of the double layer may at first move forward slightly, it generally moves back towards the plate, until eventually the double layer collapses when the anode plate is positioned just beyond the point labeled E. Overall, stable double layers are readily produced when the anode plate is located as far out as possible, although there is some indication that the magnetic field strength at the plate has to be above a minimum value. It is not clear, however, what role the apparent size of the plate has on the formation of the double layers.

F. Potential contours

Contours of constant potential which were constructed from measurements made with an axially and radially movable emissive probe are shown in Fig. 13. The contours show the formation of a low-pressure, strong, three-dimensional double layer with $e\phi/kT_e \sim 8$. The shape of these contours is similar to the visible structures described earlier and appears

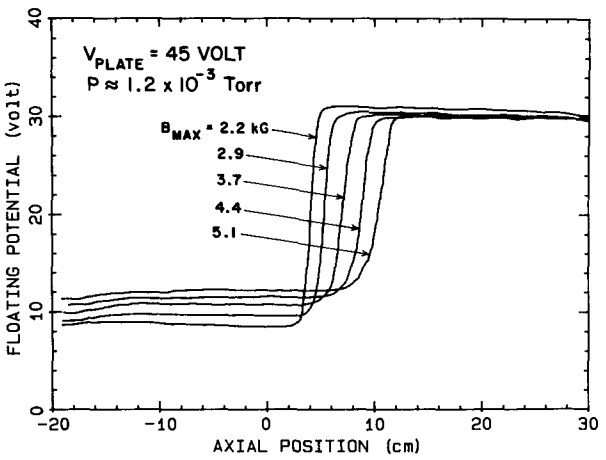

FIG. 11. Double-layer potential profiles for various overall magnetic field strengths.

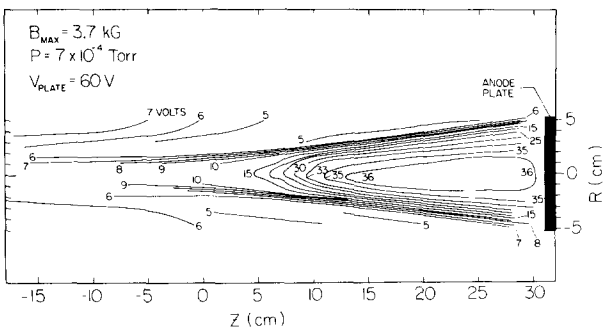

FIG. 13. Two-dimensional mapping of equipotential contours for a low-pressure double layer. The scale is 1:1.

to generally follow the diverging magnetic field lines from the anode plate. The portion of the double layer which is oblique to the magnetic field forms at axial positions from 5 to 12 cm. The magnetic field strength at $Z = 10$ cm, for example, is approximately 630 G. The one closed contour on the high-potential side of the double layer (the 36 V line) reflects a decrease in the potential occurring within 1 cm of the plate that can be as much as several volts deep. Within this contour, the potential is relatively constant. On the low-potential side, an enhancement in potential occurs along the flux tube which maps into the plate. The maximum potential in this region is 11 V. Also a slight depression of the potential (~ 1 V) is also evident on magnetic field lines just outside this flux tube. The contours in this double layer are, however, relatively gradual compared to those which form at higher pressures.

Contours of constant potential for a double layer produced at a higher pressure are shown in Fig. 14. Although the plate bias voltage is 10 V lower, the total potential across this double layer is only 2 V lower than for the case shown in Fig. 13. In this case, the potential on axis rises from 11 V on the low-potential side to a maximum of about 34 V on the high-potential side. In both cases, the magnetic field is the same. They mostly differ in the formation of the apex of the double-layer structure. The apex of the double layer shown in Fig. 14 has a squarish shape with most of the change in potential on axis occurring within a short distance of 1.5 cm. This is several times smaller than what is found in Fig. 13. Although the apex seen in Fig. 14 is located at an axial position where the magnetic field is much higher than in the previous case (i.e., 1.1 kG at $Z = 4$ cm), the increase in the thickness cannot, however, be simply a result of the difference in the magnetic field strength. In Fig. 11, the widest double layer occurs with the highest magnetic field strength. The thickness of the sides of the double layer for the two cases are much more comparable.

The variation in perpendicular thickness of the double layers shown in Figs. 13 and 14 along the magnetic field lines is shown in Fig. 15. The perpendicular thickness $\Delta L_\perp$ was obtained by measuring the distance between the 10 and 30 V contour lines shown in Figs. 13 and 14 for both positive and negative radial positions and at various axial positions. In

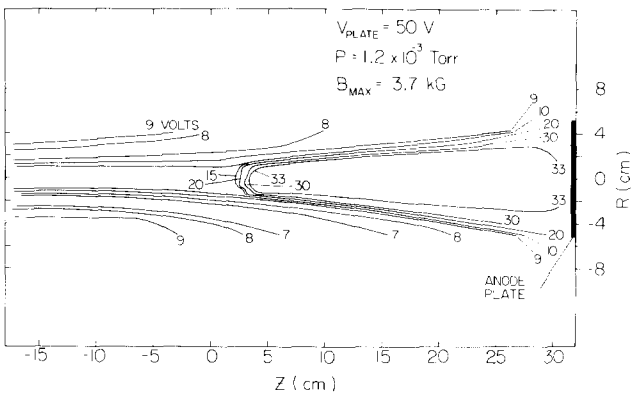

FIG. 14. Two-dimensional mapping of equipotential contours for a relatively high-pressure double layer. The scale is 1:1.

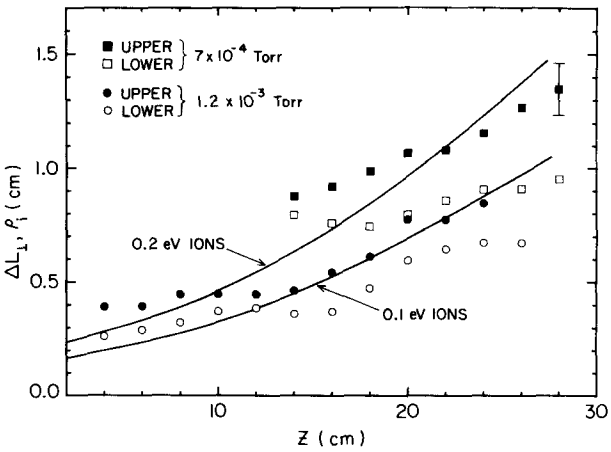

FIG. 15. Perpendicular thickness of double layers shown in Figs. 13 and 14. The data were obtained by measuring the distance between the 10 and 30 V contour lines. Solid lines indicate the local ion Larmor radius of 0.1 and 0.2 eV ions.

general, it shows that the perpendicular thickness increases with decreasing pressure and with increasing axial position. For comparison, the dependence of the Larmor radius on axial position calculated for ions having perpendicular energies of 0.1 and 0.2 eV is also shown. These energies are slightly above the energy expected for newly created ions. In both cases, the width across magnetic field lines is of the same order as the width based on the Larmor radius of cold ions; although, the mapping of the parallel component at the apex appears to be an important factor. Although curves proportional to $1/\sqrt{B}$ would fit the data more closely, the curves for the ion Larmor radii for cold ions, which are proportional to $1/B$, is shown because it can be directly compared with other scale lengths involved. In contrast, the Larmor radius of an ion at $Z = 30$ cm with a perpendicular energy of 20 eV would be 15 cm. This is even larger than the diameter of the double-layer structure.

Accompanying the formation of the double layer shown in Fig. 13 is a large density depression along magnetic field lines mapping into the anode plate, particularly where the electric field strength is greatest. Although a small density depression was already present in the center along the axis of the plasma column before the double layer was formed, the depression is greatly enhanced when the double layer is produced, as shown in Fig. 16(a) for $Z = 30$ cm. This combined with radial temperature measurements near the plate results in a variation of the Debye length from ~ 0.5 cm on the inside ($T_e \sim 10$ eV) to 0.06 cm on the outside ($T_e \sim 3$ eV). The measurements indicate that at this particular axial position $\Delta L_\perp \sim 2$ Debye lengths. In addition, the current density j_e measured with a Langmuir probe biased at the plate potential is shown in Fig. 16(b). A relatively large current flows in a narrow layer on magnetic field lines which map onto the edge of the anode plate.

G. Electron distribution functions

Measurements made with Langmuir probes also indicate that an energetic electron beam is produced on the high-

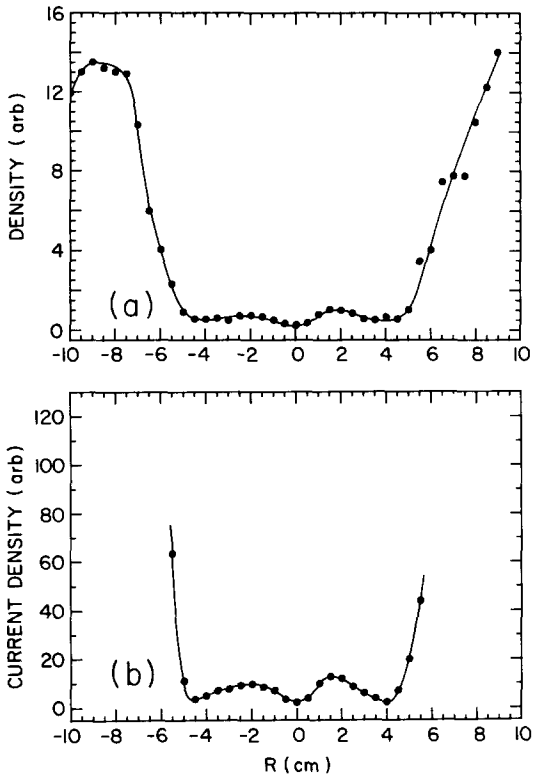

FIG. 16. Radial profiles of (a) electron density and (b) anode current density for $Z = 30$ cm (the anode plate is located at $Z = 31$ cm).

potential side of the double layers. This is shown in the bottom of Fig. 17 by measurements of the I–V probe characteristics at various axial positions ahead and behind the apex of the double-layer structure located at $Z = 6.0$ cm. These measurements were recorded at a relatively high pressure (2×10^{-3} Torr) so that the double layer would have a narrow transition region ($\Delta L_{\parallel} \approx 1$ cm) and so generate a well-defined electron beam. The beam is identified by the presence of a second knee in the probe characteristic at ~ 3.5 V, the space potential just ahead of the double layer. The derivative with respect to the bias voltage of the I–V characteristic, which is proportional to the electron distribution function [$dI/dV \sim f_e(V_{\rm pl} - V)$], is show in the top panels

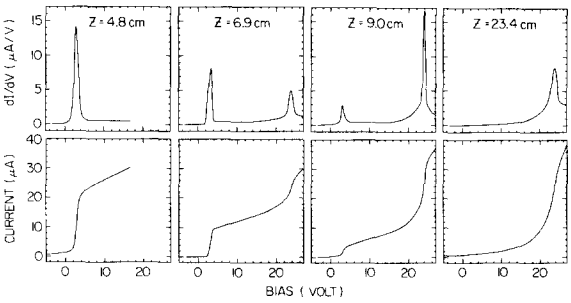

FIG. 17. Bottom: axial Langmuir probe I–V characteristic ahead ($Z = 4.8$ cm) and behind ($Z = 6.9$, 9.0, and 23.4 cm) a double layer. Top: dI/dV of the probe characteristics. A peak at ~ 3 V reflects the presence of an electron beam behind the apex of the double layer.

of Fig. 17. The measurements show that just behind the double layer, the beam accounts for most of the electron distribution. This beam rapidly thermalizes into the background plasma and is completely gone by $Z = 23.4$ cm.

In Fig. 18(a), the potentials at which the two knees in the I–V probe characteristics occur are plotted as a function of axial position, Z. The dots indicate the space potential, while the open circles indicate the potential corresponding to the second knee. The difference between the potential shown by the dots and circles indicates the peak energy of the electron beam as a function of Z. In Fig. 18(b), the total electron saturation current (background plus beam) is indicated by the dots, while the probe current, as a result of the beam alone, is indicated by the circles. In Fig. 18(c), the dependence of the apparent or bulk electron temperature

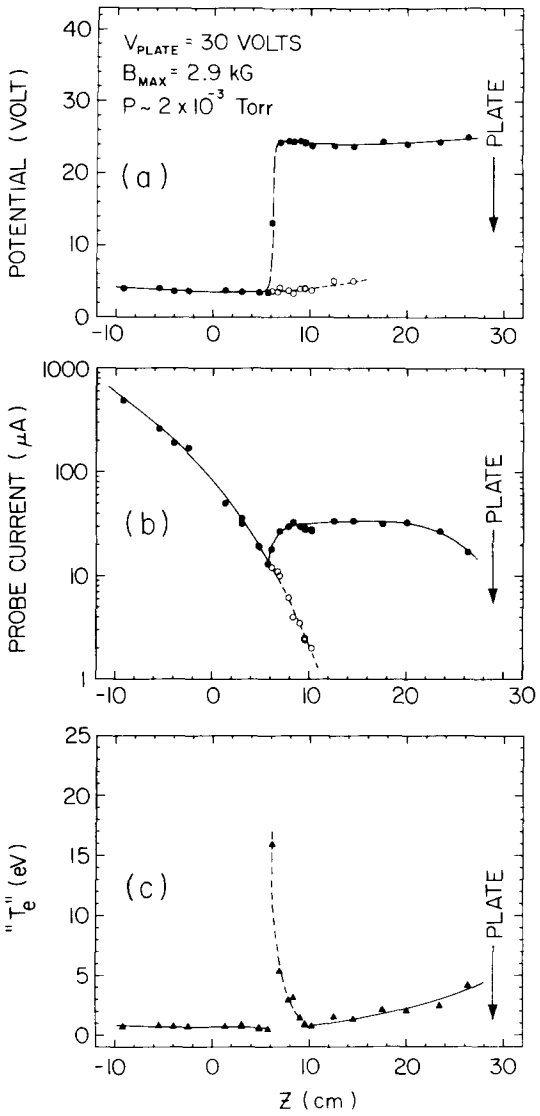

FIG. 18. Derived quantities from the probe characteristics of Fig. 17. (a) The probe potential at which the two knees occur in the probe I–V characteristics versus axial position Z. (b) The electron saturation current at the plasma space potential (dots) and the probe electron current corresponding to the electron beam (circles) versus Z. (c) The apparent or "bulk" electron temperature "T_e" vs Z.

"T_e" (eV) on position is also shown. In the region where the beam is significant, T_e appears high because it does not take into account the two-component nature of the electron distribution function as shown by Fig. 17. Overall, the figure shows that the double-layer structure is accompanied by an axial density depression with a strong axial density gradient ahead of the apex. It is also evident that the electron beam formed by the double layer decays rapidly with a relatively short e-folding length (2.2 cm in this case), and presumably contributes to the increase in the background electron temperature on the high-potential side of the double layer. Electron temperatures in excess of 10 eV have also been observed near the plate. Electron–neutral elastic collisions may be an important factor in beam thermalization, since the mean-free path for such collisions is shorter than the length of the double-layer structure. For $p \approx 2 \times 10^{-3}$ Torr, $\lambda_{en} \approx 5$ cm. Furthermore, wide-band, high-frequency plasma noise up to ~ 300 MHz, which may also be a contributing factor in the beam thermalization, was observed in the region of the electron beam. However, detailed measurements on this noise were not performed since the probe circuitry was not properly balanced for the detection of high-frequency oscillations.

IV. DISCUSSION

Strong, three-dimensional, magnetized double layers were produced in a diverging magnetic field geometry by drawing an electron current to a large, positively biased anode plate. Ionization resulting from electrons that are accelerated toward this plate is essential in maintaining a second source of plasma at a high–positive potential relative to the background plasma. The resulting production of ions neutralizes part of the negative space charge formed at the anode plate and allows a double layer to develop. By controlling this high-potential plasma by varying the neutral gas pressure and anode plate bias voltage, the formation of double layers in a nonuniform magnetic field can be studied. As V_{plate} is increased, the double layers are found to move further away from the plate and into regions of higher magnetic field strength, together with an increase in the potential across the double layer. Similarly, the length of the double-layer structures also increases with increasing neutral gas pressure. Even though the mean-free path length for ionizing collisions is on the order of a few meters (at 10^{-3} Torr), a sufficient number of ions are generated to maintain quasi-neutrality on the high-potential side. The rate at which the background neutral gas is ionized is determined in part by the double-layer potential and the distance between the double layer and the anode plate.

In addition, elastic electron–neutral collisions may be important in producing a trapped electron distribution with high pitch angles to the magnetic field within the anode plasma. Similarly, ions produced within the anode plasma will also be accelerated into the low-potential plasma ahead of the double layer. The resulting ion beam will be attenuated through charge exchange collisions. At the highest pressures used (3×10^{-3} Torr), the charge exchange mean-free path is on the order of 2 cm and is comparable to the double-layer width. Consequently, collisions should not greatly affect the distributions of particles passing through the double layers; although collisions on either side of the double layers are likely to contribute to the thermalization of the accelerated particles. Furthermore, the pitch angle distributions in a nonuniform magnetic field could also affect the formation of the double layers.

Although ionizing collisions are essential to the production of these double layers, the maximum double-layer potential $\Delta\phi_{\parallel}$ was not limited to the ionization potential (cf. Fig. 10), as observed in some experiments employing triple-plasma devices.[8] In fact, since the anode plasma is produced by ionization, these double layers generally do not appear with a potential drop less than the ionization potential of the neutral gas. Once formed the double-layer potential can be increased by increasing the anode bias voltage. The strongest double layers were produced when the anode plate was furthest from the uniform magnetic field region. Stronger double layers might have been produced if the length of the nonuniform magnetic field region had been extended.

Andersson[11] has also generated anode-type double layers but in a weak magnetic field with a slight divergence. In that experiment, the magnetic field appeared to have no decisive importance in the formation of the double layers, although it did improve their stability. In contrast to the work of Andersson[11] and to the work of Torvén and Andersson,[10] the magnetic field in our experiments is important for the formation and stability of these double layers. These double layers have regions where the potential gradient is perpendicular to the magnetic field, although oblique and parallel electric field components are clearly present. The stability of these double layers appears to arise in part because of the effect of the magnetic field on radial particle losses through the double-layer structure. In fact, Andersson and Sorensen[12] were not able to account for the transition of an anode sheath into an unmagnetized double layer by their one-dimensional model. Evidently, the stability of the solutions are affected by radial losses which would certainly be reduced in the presence of a relatively strong axial magnetic field.

In the presence of a double layer, a large density depression on the high-potential side is formed along the magnetic field lines intercepted by the anode plate. This depression results from the removal of electrons to the plate and the expulsion of ions resulting from transverse and axial potential gradients in the high-potential region. A similar density depression in the presence of anode double layers has also been observed by Stenzel *et al.*[38] Although some ions may be lost radially, a sufficient number of ions are produced to maintain quasineutrality on the high-potential side. Ions are confined radially by the strong axial magnetic field and axially, in one direction, by the high potential of the anode plate. In addition, the magnetic field divergence may reduce axial ion losses by mirror effects and provide a mechanism for stabilizing the double layers. The diverging magnetic field geometry also produces an axial density gradient in a flowing plasma with ∇n parallel to ∇B. The double layer can then regulate the supply of electrons, and hence the rate of ionization, by adjusting its axial position so as to balance plasma production and losses in a way that establishes charge neutrality on its high-potential side. This would ac-

count for the dependence of the magnetic field as shown in Fig. 11. Since the overall plasma density tends to increase at higher magnetic fields, the axial position where a stable double layer would form lies closer to the plate where the density is lower than in the main column. Alternately, at sufficiently low magnetic fields, the ion Larmor radius at the edge of the plate for even cold ions becomes so large that the high rate of ion losses prevents the establishment of charge neutrality which then leads to the collapse of these double layers.

While the parallel thickness of the double layer appears to scale with Debye length, the perpendicular thickness seems to depend on the magnetic field. Jovanović *et al.*[18] who produced double layers by injecting an electron beam into a Q machine with a uniform magnetic field, also reported a dependence of the perpendicular thickness on the magnetic field. By varying the magnetic field strength, they showed that the width of the double layers along the external magnetic field is determined by the plasma density and beam energy but in the perpendicular direction by the ion Larmor radius. In our experiment, a similar dependence was found for the scaling of the parallel potential drop, although the scaling of the perpendicular potential drop seemed to be determined by the cold ions on the high-potential side of the double layers. This may be a result of a preferential loss of ions with large perpendicular energies, leaving only the cold ions to establish the observed scaling. In addition, collisional cooling of ions with increasing neutral pressure may, in part, account for the decrease in $\Delta L_\perp$ seen between Figs. 13 and 14, although part of the double-layer structures observed here do form obliquely to the field and seem to affect the mapping of the potential along the magnetic field lines.

Another possibility is that the observed dependence of $\Delta L_\perp$ on the magnetic field reflects the spatial variation in the production of the plasma on the high-potential side of the double layers. While the ion Larmor radii along the magnetic field for cold ions are as large as ~ 2 cm, the electron Larmor radii along the magnetic field lines for even the most energetic electrons are considerably smaller. Consequently, the electrons which are accelerated by the double layers would produce new ions which lie along the same magnetic field lines. This would account for the observation that the double-layer structures are largely field aligned. This dependence would suggest that the thickness of the double layers in the direction perpendicular to the magnetic field would scale with the radius of a magnetic flux tube, i.e., with $1/\sqrt{B}$. Such a dependence is consistent with the data.

The dependence of the perpendicular thickness of the double layers reported here appears to be in contrast to the results of analytical calculations and numerical simulations found by Borovsky and Joyce[21,22] and by Borovsky.[20] They claim that for very strong double layers, the effects of the magnetic field vanish and oblique double layers follow the same scaling relation as do field-aligned or unmagnetized double layers. The results of the analytical calculations for magnetized double layers, however, assumed that the ions which were accelerated by the double layers would conserve the first adiabatic invariant.[20] Similar results were obtained in particle-in-cell numerical simulations without assuming the conservation of the first adiabatic invariant, although the effects of the particular boundary conditions used in the simulations are not clear.[20,22] In the double layers shown here, however, the invariant would be conserved only by very cold ions, since the axial distance traveled by the ions with energies much greater than 0.1 eV, during one cyclotron period, would be longer than the parallel scale lengths of the double layers.

In conclusion, the results of this work and others indicate that the presence of a nonuniform magnetic field does affect the formation and properties of double layers. It should be noted, however, that the arrangement used to generate double layers here may differ, in many respects, from those assumed in many theoretical models and simulations. For instance, the particular boundary conditions may affect the formation of double layers even when the double layers form well away from these boundaries. This is evident, for example, in the data of Fig. 9 which show that the position of the double layer can be controlled by changing the bias on the plate which can be as much as 45 cm away from the double layer. Also, the model calculations and simulations usually do not take into account the effects of collisions. It is obvious that ionizing collisions are an essential feature for the formation of these anode-type double layers. Finally, the plasma density gradients and the divergence of the magnetic field lines should be included in the models since they may also be important for understanding the formation and stability of these double layers.

ACKNOWLEDGMENTS

We wish to thank Al Scheller for his work in constructing the device and N. D'Angelo, M. Alport, J. Borovsky, C. Goertz, and G. Knorr for useful discussions.

This work was supported by the Office of Naval Research and, in part, by NASA Grant No. NGL 16-001-043.

[1] L. P. Block, Astrophys. Space Sci. **55**, 59 (1978).
[2] S. Torvén, *Wave Instabilities in Space Plasmas*, edited by P. J. Palmadesso and K. Papadopoulos (Reidel, Dordrecht, 1979), p. 109.
[3] R. A. Smith, Phys. Scr. **T2/1**, 238 (1982).
[4] N. Sato, in *Proceedings of the First Symposium on Plasma Double Layers*, edited by P. Michelsen and J. J. Rasmussen (Riso National Laboratory, Riso, Denmark, 1982), p. 116.
[5] J. E. Borovsky, in *Proceedings of the Second Symposium on Plasma Double Layers and Related Topics*, edited by R. Schrittwieser and G. Eder (University of Innsbruck, Innsbruck, Austria, 1984), p. 33.
[6] N. Hershkowitz, Space Sci. Rev. **41**, 351 (1985).
[7] P. G. Coakley and N. Hershkowitz, Phys. Fluids **22**, 1171 (1979).
[8] P. Leung, A. Y. Wong, and B. H. Quon, Phys. Fluids **23**, 992 (1980).
[9] I. R. Langmuir, Phys. Rev. **33**, 954 (1929).
[10] S. Torvén and D. Andersson, J. Phys. D **12**, 717 (1979).
[11] D. Andersson, J. Phys. D **14**, 1403 (1981).
[12] D. Andersson and J. Sorensen, J. Phys. D **16**, 601 (1983).
[13] K. D. Baker, N. Singh, L. P. Block, R. Kist, W. Kampa, and H. Thiemann, J. Plasma Phys. **26**, 1 (1981).
[14] M. Guyot and Ch. Hollenstein, Phys. Fluids **26**, 1596 (1983).
[15] S. Torvén, J. Phys. D **15**, 1943 (1982).
[16] N. Sato, R. Hatakeyama, S. Iizuka, T. Mieno, K. Saeki, J. J. Rasmussen, P. Michelsen, and R. Schrittwieser, J. Phys. Soc. Jpn. **52**, 875 (1983).
[17] R. Stenzel, M. Ooyama, and Y. Nakamura, Phys. Rev. Lett. **45**, 1498 (1980); Phys. Fluids **24**, 708 (1981).
[18] D. Jovanović, J. P. Lynov, P. Michelsen, H. L. Pécseli, J. J. Rasmussen, and K. Thomsen, Geophys. Res. Lett. **9**, 1049 (1982).
[19] W. Lennartsson, Planet. Space Sci. **28**, 135 (1980).
[20] J. E. Borovsky, Phys. Fluids **26**, 3273 (1983).
[21] J. E. Borovsky and G. Joyce, J. Geophys. Res. **88**, 3116 (1983).

[22]J. E. Borovsky and G. Joyce, J. Plasma Phys. **29**, 45 (1983).
[23]J. E. Borovsky, J. Geophys. Res. **89**, 2251 (1984).
[24]D. J. Gorney, A. Clarke, D. Croley, J. Fennell, J. Luhmann, and P. Mizera, J. Geophys. Res. **86**, 83 (1981).
[25]E. Ungstrup, D. M. Klumpar, and W. J. Heikkila, J. Geophys. Res. **84**, 4289 (1979).
[26]D. W. Swift, J. Geophys. Res. **84**, 6427 (1979).
[27]F. S. Mozer, C. W. Carlson, M. K. Hudson, R. B. Torbert, B. Parady, J. Yatteau, and M. C. Kelley, Phys. Rev. Lett. **38**, 292 (1977).
[28]N. Singh, R. W. Schunk, and H. Thiemann, Adv. Space Res. **4**, 481 (1984).
[29]W. Lennartsson, in *Proceedings of the Chapman Conference on Ion Acceleration in the Magnetosphere and Ionosphere*, AGU Monograph Series 38 (AGU, Washington, D.C., 1986), p. 323.
[30]J. S. Wagner, J. R. Kan, S.-I. Akasofu, T. Tajima, J. N. Leboeuf, and J. M. Dawson, *Physics of Auroral Arc Formation*, AGU Monograph Series 25 (AGU, Washington, D.C., 1981), p. 304.
[31]J. S. Levine and F. W. Crawford, J. Plasma Phys. **24**, 359 (1980).
[32]R. Hatakeyama, Y. Suzuki, and N. Sato, Phys. Rev. Lett. **50**, 1203 (1983).
[33]M. Nakamura, R. Hatakeyama, and N. Sato, in *Proceedings of the Second Symposium on Plasma Double Layers and Related Topics*, edited by R. Schrittwieser and G. Eder (University of Innsbruck, Innsbruck, Austria, 1984), p. 171.
[34]R. L. Merlino, S. L. Cartier, M. J. Alport, and G. Knorr, in *Proceedings of the Second Symposium on Plasma Double Layers and Related Topics*, edited by R. Schrittwieser and G. Eder (University of Innsbruck, Innsbruck, Austria, 1984), p. 224.
[35]M. J. Alport, S. L. Cartier, and R. L. Merlino, J. Geophys. Res. **91**, 1599 (1986).
[36]J. B. Hasted, *Physics of Atomic Collisions*, 2nd ed. (Elsevier, New York, 1972); J. C. Nickel, K. Imre, O. F. Register, and S. Trajmar, J. Phys. B **18**, 125 (1985).
[37]R. L. Merlino and S. L. Cartier, J. Phys. D, in press.
[38]R. L. Stenzel, W. Gekelman, and N. Wild, J. Geophys. Res. **88**, 4793 (1983).